3D Magnetic Susceptibility Correction with Application to Diffusion-Weighted Imaging

A. T. Van[1], and B. P. Sutton[2]

[1]Electrical and Computer Engineering, University of Illinois at Urbana-Champaign, Urbana, IL, United States, [2]Bioengineering, University of Illinois at Urbana-Champaign, Urbana, IL, United States

INTRODUCTION

Three-dimensional diffusion-weighted imaging (DWI) is time-consuming due to the large number of required sampled *k*-space points for full 3D encoding and the wait for T1 recovery between consecutive acquisitions. To reduce the total scan time, acquisitions with long readout duration are usually used. Additionally, in multishot DWI, to minimize the potential for local undersampling resulting from motion-induced phase errors, oversampled trajectories should be used. The oversampled or variable density trajectories can further increase the readout duration. Therefore, even with a spin echo preparation, magnetic susceptibility artifacts are significant in 3D DWI. The current study proposes to correct for the magnetic susceptibility artifacts in 3D DWI by incorporating the effect into the 3D encoding matrix and solving the inverse problem iteratively. The current method is based on a previously proposed algorithm [1]. *In vivo* results show the effectiveness of the method in minimizing the magnetic susceptibility artifacts.

METHOD

The received signal under the effect of magnetic susceptibility can be modeled as [1]:

$$y(t_m) = \sum_{n=0}^{N-1} f(\mathbf{r}_n) \exp\left(j\omega(\mathbf{r}_n)t_m - 2\pi \mathbf{k}(t_m)\cdot\mathbf{r}_n \right) \qquad (1)$$

$$m = 0, 1, \ldots, M-1$$

where $f(\mathbf{r}_n)$ and $\omega(\mathbf{r}_n)$ are the parameterized 3D imaging object and 3D field map, respectively, t_m is the acquisition time of the m^{th} *k*-space point, and $\mathbf{k}$ is the 3D designed *k*-space trajectory. Equation (1) can be rewritten in matrix form as:

$$\mathbf{y} = \mathbf{Af} + \boldsymbol{\varepsilon} \qquad (2)$$

where $\mathbf{y} = [\, y(t_0) \quad y(t_1) \quad \ldots \quad y(t_{M-1}) \,]^T$, $\mathbf{f} = [\, f(r_1) \quad f(r_2) \quad \ldots \quad f(r_{N-1}) \,]$, $\boldsymbol{\varepsilon}$ is the vector of measurement noise, and $\mathbf{A}$ is the *MxN* encoding matrix with entries

$$a_{m,n} = \exp\left(j\omega(\mathbf{r}_n) - j2\pi \mathbf{k}(t_m)\cdot\mathbf{r}_n \right) \qquad (3)$$

Assume that the noise is additive white Gaussian, the maximum likelihood estimation of **f** is achieved by minimizing the cost function

$$\Psi(\mathbf{f}) = \left\| \mathbf{y} - \mathbf{Af} \right\|_2^2 \qquad (4)$$

To speed up the reconstruction, a combination of nonuniform fast Fourier transform (NUFFT) [2] and time-segmented approach [1] was applied in solving Equation (4).

<u>*Data Acquisition:*</u> A 3D multislab [3] stack of six-shot variable density spirals [4] with 3D navigator acquisition was used. *In vivo* data were acquired using Siemens 3 T Trio scanner with a 12-channel head coil on a healthy subject in accordance with the institutional review board. The obtained resolution was 1.88 x 1.88 x 2 mm^3 with 24 x 24x15cm^3 field-of-view. The readout duration per spiral shot was 20 ms. Other imaging parameters include: TE1 = 64 ms (for data), TE2 = 110 ms (for navigator), navigator matrix size = 15 x 15 x 10, and b = 1000 s/mm^2. The acquisition was cardiac-gated for enhancement of the rigid body motion assumption resulting in an effective TR of two R-R intervals (approximately 2 s). Field map at the same spatial resolution was acquired separately using a gradient echo sequence.

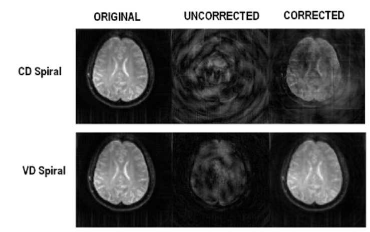

Fig. 1: The necessity of oversampling in multishot DWI. After phase correction, CD spiral still gives ghosting (first row) while VD spiral restores the original image (second row).

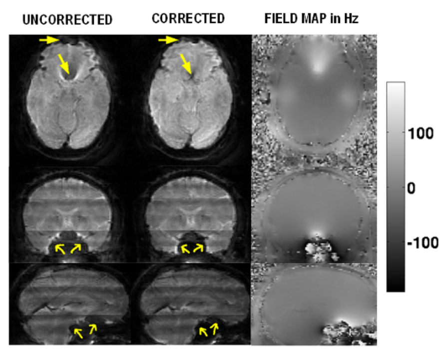

Fig. 2: b = 0 images with and without magnetic susceptibility correction. The field maps are in Hz.

RESULTS

<u>*Simulation*</u>*:* A simulation study was done to show the necessity of oversampling in multishot DWI. Random *k*-space shifts and phase offsets were added to *k*-space data from each shot to simulate the effect of rigid-body-motion-induced phase errors [5]. Even after correction with the exact phase error parameters, the data simulated with the constant density spiral trajectory still shows significant ghosting (Fig. 1, first row). Only with the variable density spiral trajectory with oversampling factor $\alpha = 4$ does the corrected image restores the original simulated phantom (Fig. 1, second row). However, this oversampling increases the readout duration and sensitivity to magnetic susceptibility effects.

<u>*In Vivo*</u>: Fig. 2 and Fig. 3 show the field maps used and the obtained b = 0 and diffusion-weighted images with and without magnetic susceptibility correction. Without correction, distortion is severe especially in the regions pointed to by the arrows. Correction puts the signals back to where they belong and significantly improves the quality of the image.

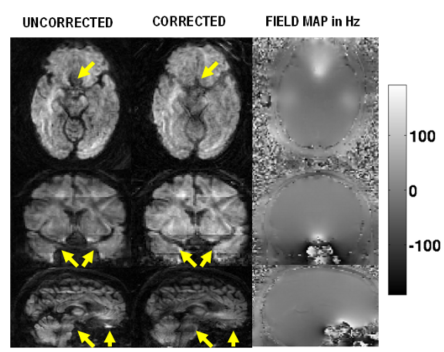

Fig. 3: Diffusion-weighted images with and without magnetic susceptibility correction. The field maps are in Hz.

DISCUSSION and CONCLUSION

With a true 3D trajectory and 3D field inhomogeneity, the total reconstruction time even with NUFFT and time segmentation is rather long. Parallelization of the reconstruction on a cluster or using graphics processing units (GPUs) will bring the reconstruction time down to an acceptable time.

Parallel imaging is another approach to reduce the magnetic susceptibility artifacts. However, in the case of 3D DWI, it is preferable to use parallel imaging for speeding up the relatively long acquisition, leaving the magnetic susceptibility correction for post processing.

The current work has shown the necessity of magnetic susceptibility correction in 3D DWI. Based on a previously proposed algorithm, we have developed and applied a truly 3D magnetic susceptibility correction to *in vivo* 3D DWI.

REFERENCES

[1] Sutton et al, IEEE TMI. 22: p178-188, 2003; [2] Fessler et al, IEEE TSP. 51: p560-574, 2003; [3] Van et al, ISMRM 2010, p1618; [4] Kim et al, MRM. 50: p214-219, 2003; [5] Van et al, IEEE TMI. 28: p1770-1780, 2009.

ACKNOWLEDGEMENTS – This work was supported by an AFAR research grant**.**